4-Nitrobenzaldehyde thiosemicarbazone: a new compound derived from *S*-(-)-limonene that induces mitochondrial alterations in epimastigotes and trypomastigotes of *Trypanosoma cruzi*

ELIZANDRA APARECIDA BRITTA[1], DÉBORA BOTURA SCARIOT[1], HUGO FALZIROLLI[2], CLEUZA CONCEIÇÃO DA SILVA[2], TÂNIA UEDA-NAKAMURA[1], BENEDITO PRADO DIAS FILHO[1], REDOUANE BORSALI[3] *and* CELSO VATARU NAKAMURA[1]*

[1] *Programa de Pós-graduação em Ciências Farmacêuticas, Universidade Estadual de Maringá, PR, Avenida Colombo, 5790, Jd. Universitário, Maringá, Paraná 87020-900, Brazil*
[2] *Departamento de Química, Universidade Estadual de Maringá, Maringá, PR, Avenida Colombo, 5790, Jd. Universitário, Maringá, Paraná 87020-900, Brazil*
[3] *Univ. Grenoble Alpes, CERMAV-CNRS UPR 5301, F-38000 Grenoble, France*

(*Received 5 November 2014; revised 19 January 2015; accepted 20 January 2015; first published online 25 February 2015*)

SUMMARY

Trypanosoma cruzi is the causative agent of Chagas' disease, a parasitic disease that remains a serious health concern with unsatisfactory treatment. Drugs that are currently used to treat Chagas' disease are partially effective in the acute phase but ineffective in the chronic phase of the disease. The aim of the present study was to evaluate the antitrypanosomal activity and morphological, ultrastructural and biochemical alterations induced by a new molecule, 4-nitrobenzaldehyde thiosemicarbazone (BZTS), derived from *S*-(-)-limonene against epimastigote, trypomastigote and intracellular amastigote forms of *T. cruzi*. BZTS inhibited the growth of epimastigotes (IC_{50} = 9·2 μM), intracellular amastigotes (IC_{50} = 3·23 μM) and inhibited the viability of trypomastigotes (EC_{50} = 1·43 μM). BZTS had a CC_{50} of 37·45 μM in $LLCMK_2$ cells. BZTS induced rounding and distortion of the cell body and severely damaged parasite mitochondria, reflected by extensive swelling and disorganization in the inner mitochondrial membrane and the presence of concentric membrane structures inside the organelle. Cytoplasmic vacuolization, endoplasmic reticulum that surrounded organelles, the loss of mitochondrial membrane potential, and increased mitochondrial $O_2^{\cdot-}$ production were also observed. Our results suggest that BZTS alters the ultrastructure and physiology of mitochondria, which could be closely related to parasite death.

Key words: *Trypanosoma cruzi*, antitrypanosomal activity, 4-nitrobenzaldehyde thiosemicarbazone, mitochondria alterations, cell death.

INTRODUCTION

Chagas' disease is caused by *Trypanosoma cruzi* and represents an important health problem in Latin America, where it affects approximately 7–8 million people (World Health Organization, 2014). Chagas' disease presents chronic and severe clinical complications in the heart and digestive system. Neurological disorders that are caused by *T. cruzi* infection have also been described in children and immunosuppressed hosts (Bombeiro *et al*. 2012). The transmission of Chagas' disease to the vertebrate host occurs through the penetration of trypomastigotes, which are eliminated in the feces and urine of triatomines, at the bite site during blood feeding. Alternatively, infection can occur through other routes, such as congenital transmission, blood transfusion, organ transplantation, oral transmission and laboratory accidents (Álvarez *et al*. 2014; Kransdorf *et al*. 2014; Vannucchi *et al*. 2014). *Trypanosoma cruzi* can be found in the vertebrate host as the amastigote form that is strictly intracellular and proliferative. Epimastigotes have a tapered body with a long and extensive scourge, proliferate and undergo an intense phase of cell division in the triatomine gut. Extracellular trypomastigotes are stationary and infective and circulate freely in the blood and tissue of the vertebrate host. In the invertebrate host, they are found in the final portion of the digestive tract, feces and urine (De Souza *et al*. 2010; Álvarez *et al*. 2014).

Chemotherapeutic strategies that are currently employed for Chagas' disease remain inefficient. The available treatments are unable to suppress *T. cruzi* infection or permanently cure all patients.

* Corresponding author. Programa de Pós-graduação em Ciências Farmacêuticas, Universidade Estadual de Maringá, PR, Avenida Colombo, 5790, Jd. Universitário, Maringá, Paraná 87020-900, Brazil. E-mail: cvnakamura@uem.br

Parasitology (2015), **142**, 978–988.
doi:10.1017/S0031182015000141

Benznidazole and nifurtimox are the drugs that are currently used to treat Chagas' disease, but they are only partially effective in the acute phase and ineffective in the chronic phase of the disease (Cerecetto and González, 2002; Coura and De Castro, 2002).

Our group recently reported the antileishmania activity of a novel molecule, 4-nitrobenzaldehyde thiosemicarbazone (BZTS – $C_{19}H_{24}O_2N_4S$), derived from *S*-(-)-limonene, against the promastigote, axenic amastigote and intracellular amastigote forms of *Leishmania amazonensis*. We found that BZTS induced marked effects on the morphology and ultrastructure of the parasite, including interference with various cellular processes that led to changes in shape and mitochondrial function, the accumulation of lipid droplets, and evidence of apoptotic and autophagic processes (Britta *et al*. 2014). The aim of the present study was to investigate the antiproliferative, ultrastructural and physiological effects of BZTS on epimastigotes and trypomastigotes of *T. cruzi*. The results showed that BZTS induced alterations principally in the ultrastructure and physiology of mitochondria, which could be closely related to parasite death.

MATERIALS AND METHODS

Chemicals

Carbonyl cyanide m-chlorophenylhydrazone (CCCP), digitonin, dimethylsulphoxide (DMSO), antimycin A and rhodamine 123 (Rh123) were purchased from Sigma-Aldrich (St. Louis, MO, USA). Fetal bovine serum (FBS) was obtained from Invitrogen (Grand Island, NY, USA). 3,8-Phenanthridinediamine-5-(6-triphenylphosphonium hexyl)-5,6-dihydro-6-phenyl (MitoSOX) and propidium iodide (PI) were obtained from Invitrogen (Eugene, OR, USA). All of the other reagents were of analytical grade.

Synthesis of BZTS derived from S-(-)-limonene

BZTS was synthesized as described by Britta *et al*. (2014).

Parasites and LLCMK$_2$ cell cultures

Epimastigote forms of *T. cruzi* (Y strain) were axenically maintained at 28 °C in Liver Infusion Tryptose (LIT) medium, pH 7·4, supplemented with 10% heat-inactivated FBS for 96 h. Trypomastigote forms were obtained from the supernatants of previously infected monolayers of LLCMK$_2$ (i.e. epithelial cells of monkey kidney) cells in Dulbecco's modified Eagle medium (DMEM; Gibco Invitrogen, Grand Island, NY, USA). LLCMK$_2$ cells were maintained in DMEM supplemented with 2 mM L-glutamine, 10% FBS, and 50 mg L^{-1} gentamicin and buffered with sodium bicarbonate in a 5% CO_2 air mixture at 37 °C.

Antiproliferative activity of BZTS against epimastigote forms

Epimastigote forms of *T. cruzi* in the logarithmic phase (1×10^6 parasites mL^{-1}) were grown in 24-well culture microplates at 28 °C in LIT medium supplemented with 10% FBS. BZTS was dissolved in DMSO and LIT medium to final concentrations of 2·7, 13·9, 27·7, 139 and 277 μM. The final concentration of DMSO did not exceed 1%, which has no deleterious effects on the parasites. The antiproliferative activity of BZTS was determined by directly counting free-living parasites in a Neubauer chamber, and the concentration that inhibited growth by 50% (IC_{50}) and 90% (IC_{90}) was determined by regression analysis of the data.

Effects of BZTS on trypomastigote viability

Trypomastigotes that were obtained from the supernatant of infected LLCMK$_2$ cells were inoculated (1×10^7 parasites mL^{-1}) in DMEM and added to 96-well plates in the presence of increasing concentrations of BZTS (0·27, 2·77, 13·9 and 27·7 μM). The parasites were incubated for 24 h at 37 °C in a 5% CO_2 atmosphere. After incubation, viability of the parasites was determined by examining mobility under an Olympus CX31 light microscope. A 5 μL aliquot of each sample was placed on slides. The slides were coverslipped, and the parasites were immediately counted. The effective concentrations that lysed 50% (EC_{50}) and 90% (EC_{90}) of the parasite were calculated by regression analysis of the data.

Effects of BZTS on intracellular amastigote forms

Sterile glass coverslips were placed in the wells of a 24-well microplate, and $2{\cdot}5 \times 10^5$ cells mL^{-1} were added to each well in DMEM medium supplemented with 10% FBS. The microplate was incubated for 24 h at 37 °C in a 5% CO_2-air mixture to adhere cells. The cell monolayer was infected with trymastigote forms at a 10:1 parasite:cell ratio. After 24 h of interaction at 37 °C in a 5% CO_2-air mixture, the microplate was washed with phosphate-buffered saline (PBS) to remove the non-interiorized parasites. Afterward, the infected LLCMK$_2$ cells were treated with BZTS at concentrations of 2·7, 13·8 and 27·7 μM and incubated for 96 h. The coverslip was fixed with methanol, Giemsa-stained and permanently mounted. A total of 200 cells were counted using an optical microscope, and the percentage of infected cells and number of intracellular parasites were estimated. The survival index was calculated as the product of

https://doi.org/10.1017/S0031182015000141 Published online by Cambridge University Press

the percentage of infected cells and the number of amastigotes per cell. The IC_{50} and IC_{90} were determined by regression analysis.

In vitro cytotoxicity assay of BZTS against LLCMK$_2$ cells

$LLCMK_2$ cell monolayers were suspended to yield 5×10^5 cells mL^{-1} in DMEM medium supplemented with 10% FBS and added to each well of 96-well microtiter plates. The plates were incubated in a 5% CO_2-air mixture at 37 °C for 24 h to obtain confluent cell monolayers. The monolayers were then treated with different concentrations of BZTS (2·7, 13·9, 27·7, 139 and 277 μM) for 96 h. After treatment, the $LLCMK_2$ cell monolayers were washed with PBS, and 50 μL of MTT (3-[4,5-dimethylthiazol-2-yl]-2,5-diphenyltetrazolium bromide formazan; 2 mg mL^{-1}) solution was added. The microplate was incubated for 4 h in a 5% CO_2-air mixture at 37 °C, and 150 μL of DMSO was added. Absorbance was read in a microplate reader (BIO-TEK Power Wave XS) at 570 nm. The percentage of viable cells was calculated compared with controls (i.e. cells cultured in medium without drug). The 50% cytotoxic concentration (CC_{50}) was determined by regression analysis of the data.

Morphological analysis by scanning electron microscopy (SEM)

Epimastigote forms were treated with concentrations that corresponded to the IC_{50} and IC_{90} of BZTS for 96 h at 28 °C. The parasites were fixed in 2·5% glutaraldehyde in 0·1 M sodium cacodylate buffer for 1–3 h. Parasites were adhered on poly-L-lysine-coated coverslips and dehydrated in an ascending series of ethanol. The samples were critical-point-dried in CO_2, coated with gold, and observed in a Shimadzu SS-550 scanning electron microscope.

Ultrastructural analysis by transmission electron microscopy (TEM)

Epimastigote forms were treated with concentrations that corresponded to the IC_{50} and IC_{90} of BZTS for 96 h at 28 and 32 °C, respectively. After washing with PBS, the parasites were fixed in 2·5% glutaraldehyde in 0·1 M sodium cacodylate buffer at 4 °C and post-fixed in a solution that contained 1% osmium tetroxide, 0·8% potassium ferrocyanide and 5 mM calcium chloride. The parasites were dehydrated in an acetone series and embedded in Epon resin for 72 h at 60 °C. Ultrathin sections were stained with 5% uranyl acetate and lead citrate and examined in a JEOL JEM 1400 transmission electron microscope.

Evaluation of the integrity of the cell membrane

Epimastigote forms of *T. cruzi* (1×10^7 cells mL^{-1}) were exposed to 139, 277, and 555 μM BZTS for 24 h at 25 °C and then harvested and washed with PBS. The parasites were incubated with 50 μL of 2 mg mL^{-1} PI for 5 min according to the manufacturer's instructions. Immediately thereafter, the cells were analysed using a BD FACSCalibur flow cytometer equipped with CellQuest Pro software. A total of 10 000 events were acquired in the region that corresponded to the parasites. Alterations in PI fluorescence were determined compared with untreated parasites. Digitonine (40·0 μM) was used as a positive control.

Determination of mitochondrial transmembrane potential ($\Delta\Psi m$)

Epimastigotes (1×10^7 cells mL^{-1}) were exposed to 139, 277 and 555 μM BZTS for 24 h at 28 °C, and trypomastigotes were treated with 27·7, 55·5 83·2 μM BZTS. The cells were then incubated with 1 μL (5 mg mL^{-1} in ethanol) of rhodamine 123 (Rh123; Sigma-Aldrich, St. Louis, MO, USA) for 15 min, resuspended in 0·5 mL PBS, and incubated for an additional 30 min. The assay was conducted according to the manufacturer's instructions. The parasites were analysed using a BD FACSCalibur flow cytometer and CellQuest Pro software. A total of 10 000 events were acquired in the region that corresponded to the parasites. CCCP (100·0 μM) was used as a positive control. Alterations in Rh123 fluorescence were evaluated as a decrease in the gated percentage in the upper-right quadrant and increase in the gated percentage in the low-left quadrant.

Determination of mitochondrial superoxide anion radicals ($O_2^{\bullet-}$)

Epimastigote and trypomastigote forms were harvested and washed with Krebs–Henseleit (KH) solution buffer, pH 7·3, that contained 15 mM $NaHCO_3$, 5 mM KCl, 120 mM NaCl and 0·7 and 1·5 mM NaH_2PO_4. The cells were loaded with 2·0 mL of 5 μM MitoSOX reagent (3,8-phenanthridinediamine-5-[6-triphenylphosphoniumhexyl]-5,6-dihydro-6-phenyl). The parasites were incubated for 10 min at 37 °C and protected from light. After incubation with MitoSOX reagent, the parasites were washed three times with KH buffer and treated with BZTS. Epimastigotes were treated with 55, 139, 277 and 555 μM, and trypomastigotes were treated with 27·7, 55·5, 83·2 and 139 μM. Antimycin A (10 μM) was used as a positive control. MitoSOX detection was performed using black 96-well plates for 6 h. Fluorescence was measured at excitation and emission wavelengths of 510 and 580 nm, respectively, in a VICTOR X3

https://doi.org/10.1017/S0031182015000141 Published online by Cambridge University Press

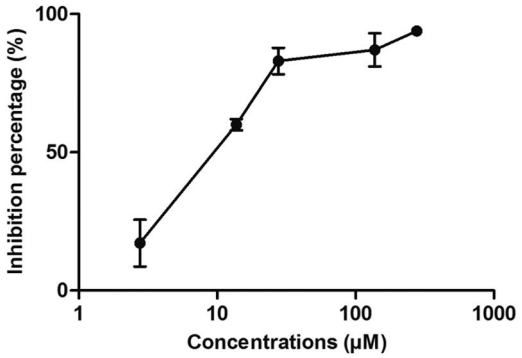

Fig. 1. Inhibition percentage of epimastigote forms of *T. cruzi* treated with BZTS for 96 h. The data are expressed as the means from three independent experiments.

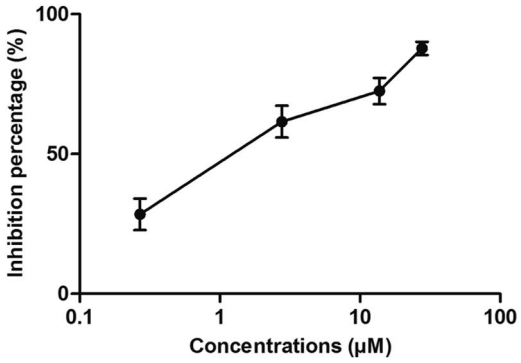

Fig. 2. Viability inhibition percentage of trypomastigote forms of *T. cruzi* treated with BZTS for 24 h. The data are expressed as the means from three independent experiments.

spectrofluorometer (Perkin Elmer). The results are expressed as arbitrary units of MitoSOX.

Statistical analysis

The data are expressed as the mean ± standard deviation (S.D.) of at least three independent experiments. The data were analysed using one- and two-way analysis of variance (ANOVA). Significant differences among means were identified using the Tukey and Bonferroni *post hoc* tests. Values of $P \leq 0{\cdot}05$ were considered statistically significant. The statistical analyses were performed using GraphPad Prism 5 software.

RESULTS

Antiproliferative effects of BZTS on epimastigote and intracellular amastigote forms, trypomastigote viability and LLCMK$_2$ cell cytotoxicity

Treatment of the parasites with BZTS dose-dependently inhibited growth of the epimastigote forms after 96 h incubation with increasing concentrations (2·7, 13·9, 27·7, 139 and 277 μM). The IC_{50} and IC_{90} were 9·2 ± 1·7 μM and 44·4 ± 18·2 μM, respectively (Fig. 1). To determine the effects of BZTS on trypomastigote viability, the parasites were treated for 24 h with 0·27, 2·77, 13·9 and 27·7 μM concentrations, and the effective concentrations that lysed 50% (EC_{50}) and 90% (EC_{90}) of the parasites were calculated. The EC_{50} and EC_{90} were 1·43 ± 0·9 μM and 26·8 ± 1·6 μM, respectively (Fig. 2). In the intracellular amastigotes, the IC_{50} and IC_{90} were 3·23 ± 0·6 μM and 11·84 ± 0·2 μM, respectively. In the concentrations of 13·8 and 27·7 μM BZTS viability of amastigotes were 0·0%, and at 2·7 μM BZTS viability of amastigotes was 52·83%. These results demonstrate that BZTS was more effective against the trypomastigote form than the epimastigote form. To evaluate the cytotoxic effect of BZTS, LLCMK$_2$ cells were treated with different concentrations of BZTS and evaluated using the MTT method. The CC_{50} was

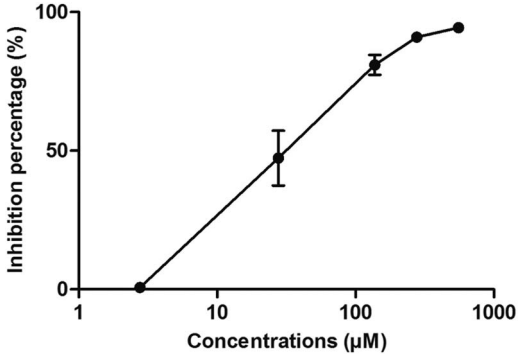

Fig. 3. Inhibition percentage of LLCMK$_2$ cells after treatment with BZTS for 96 h. The data are expressed as the means from three independent experiments.

37·45 ± 6·6 μM after 96 h treatment (Fig. 3). The CC_{50} was compared with the activity against epimastigotes (IC_{50}), trypomastigotes (EC_{50}) and intracellular amastigotes (IC_{50}), yielding the selectivity index (SI; ratio of the CC_{50} in LLCMK$_2$ cells to the IC_{50} and EC_{50} in protozoa). BZTS was more toxic to the protozoa than to LLCMK$_2$ cells (SI = 4·1 for epimastigotes; SI = 26·2 for trypomastigotes and SI = 11·6 for intracellular amastigotes).

SEM and TEM

The SEM analysis showed that untreated parasites presented normal characteristics, with an elongated shape and free flagellum, and BZTS caused morphological alterations in the shape and size of the parasites. These alterations were more pronounced in parasites that were treated with the IC_{90} (44·4 μM) of BZTS, which showed rounding and distortions of the cell body (Fig. 4). TEM showed that untreated parasites exhibited a normal ultrastructure of organelles, including mitochondria, kinetoplasts, nuclei and reservosomes. The treatment of epimastigotes with BZTS led to severe damage of mitochondria, reflected by extensive swelling and

https://doi.org/10.1017/S0031182015000141 Published online by Cambridge University Press

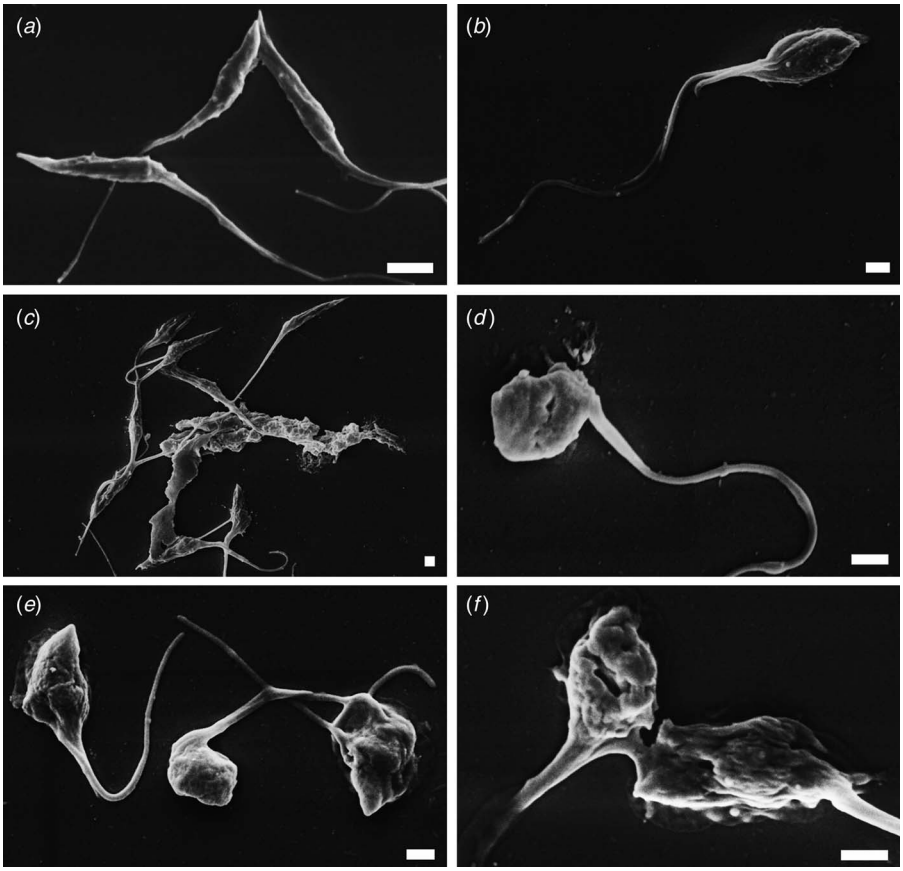

Fig. 4. SEM of *T. cruzi*. The figure shows control epimastigotes (A) and epimastigotes treated with the IC_{50} (B, C) and IC_{90} (D, F) of BZTS. Scale bar = 1 μM.

disorganization of the inner mitochondrial membrane and the presence of concentric membrane structures inside the organelle. Cytoplasmic vacuolization and the appearance of an endoplasmic reticulum that surrounded organelles were also observed (Fig. 5).

Evaluation of cell membrane integrity

Alterations in cell membrane integrity were evaluated in epimastigotes treated with BZTS using PI staining, which is a nucleic acid stain that penetrates cells with a compromised plasma membrane and does not cross the membranes of live cells. BZTS-treated epimastigotes did not show permeabilization of the plasma membrane compared with untreated parasites. The treatment of epimastigotes with BZTS at 139, 277 and 555 μM caused a gated percentage of PI-stained parasites of 1·07 ± 0·3%, 1·35 ± 0·7% and 1·47 ± 0·5%, respectively (Fig. 6C–E, upper-left quadrant). Untreated epimastigotes had a similar gated percentage of 0·87 ± 0·3% (Fig. 6A, upper-left quadrant). In contrast, epimastigotes treated with digitonin (40·0 μM) exhibited an increase in the gated percentage of PI-stained cells of 92·59 ± 5·3% (Fig. 6B, upper-left quadrant).

Determination of mitochondrial transmembrane potential ($\Delta\Psi m$)

The analysis of mitochondrial transmembrane potential ($\Delta\Psi$m) using flow cytometry showed that BZTS induced a considerable loss of the $\Delta\Psi$m in both the epimastigote and trypomastigote forms of *T. cruzi*. Figures 7 and 8 show a decrease in the gated percentage in the upper-right quadrant and an increase in the gated percentage in the low-left quadrant, demonstrating a reduction of $\Delta\Psi$m. When epimastigotes labelled with Rh123 were treated with 139, 277 and 555 μM BZTS, the gated percentages in the low-left quadrant were 40·97, 63·06, and 80·91%, respectively. Parasites that were treated with CCCP as a positive control exhibited a 77·66% decrease in $\Delta\Psi$m, whereas untreated parasites exhibited a 1·71% decrease (Fig. 7). Similarly, 76·22, 93·10 and 81·35% of the trypomastigotes that were treated with 27·7, 55·5 and 83·2 μM BZTS were positive for Rh123, respectively. Parasites that were treated with CCCP as a positive control exhibited a 81·12% decrease in $\Delta\Psi$m, whereas untreated parasites showed a 13·35% decrease in $\Delta\Psi$m (Fig. 8). These results demonstrate that BZTS decreased the Rh123 fluorescence intensity.

https://doi.org/10.1017/S0031182015000141 Published online by Cambridge University Press

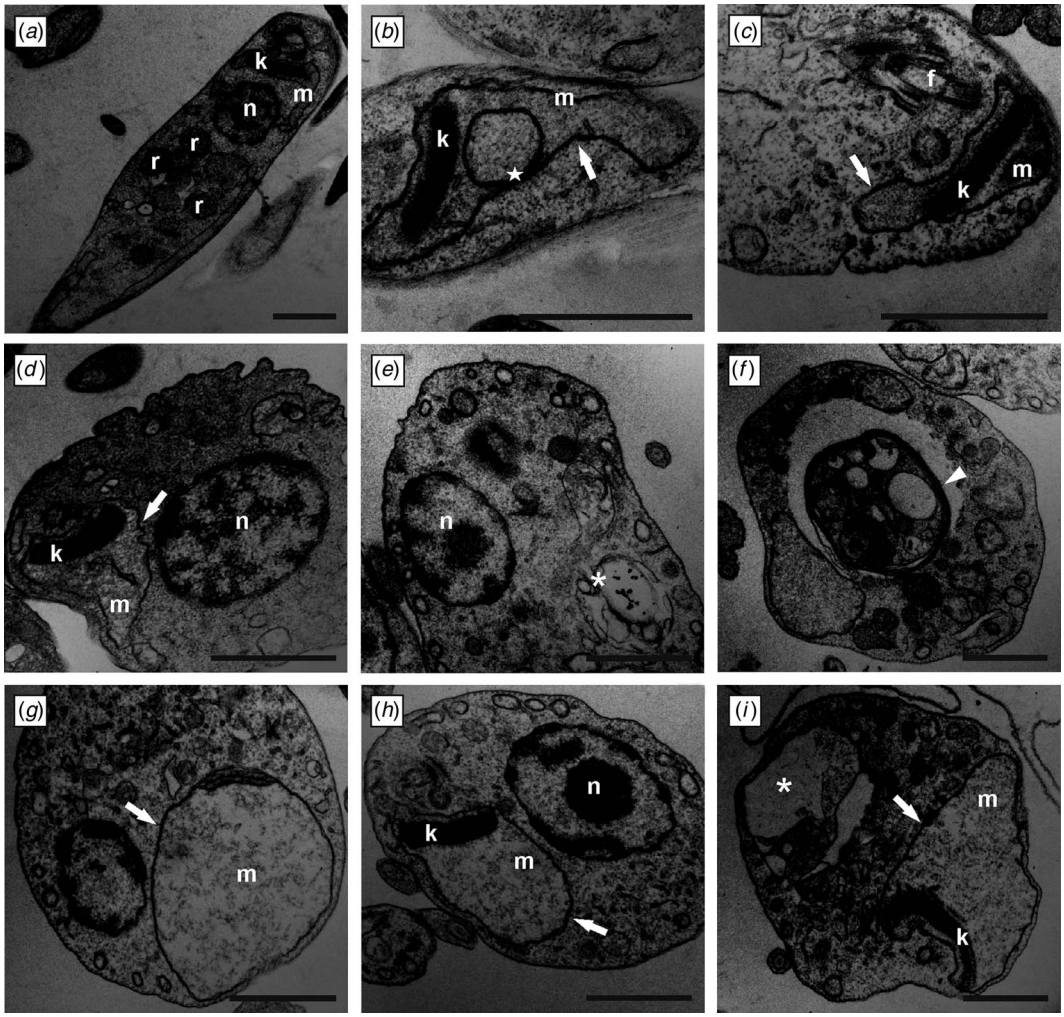

Fig. 5. TEM of *T. cruzi* epimastigotes. The figure shows control epimastigotes (A) and epimastigotes treated with the IC_{50} (B–D) and IC_{90} (E, I) of BZTS. White arrows indicate mitochondrial swelling. The asterisk indicates cytoplasmic vacuolization. The star indicates membranous structures inside mitochondria. The white arrowhead indicates endoplasmic reticulum surrounding organelles. n, nuclei; m, mitochondrion; k, kinetoplast; r, reservosome. Scale bar = 1 μM.

Production of mitochondrial superoxide anion radicals ($O_2^{\bullet-}$)

Based on our $\Delta\Psi$m results, we evaluated $O_2^{\bullet-}$ production in epimastigotes and trypomastigotes that were treated with BZTS using MitoSOX reagent, which is accumulated in mitochondria based on its hydrophobic nature and positively charged triphenylphosphonium moiety. Figures 9 and 10 show that BZTS increased mitochondrial $O_2^{\bullet-}$ production in epimastigotes and trypomastigotes at most of the concentrations and times tested compared with the control group. After 1 h of treatment, epimastigotes that were treated with 277 and 555 μM BZTS exhibited a significant increase in $O_2^{\bullet-}$ production. In protozoa that were treated with 139 μM BZTS, the increase was significant after 2 h of treatment, and the 55 μM concentration was significant after 4 h of treatment (Fig. 9). Trypomastigotes that were treated with 27·7, 55, 83·2 and 139 μM BZTS exhibited significant $O_2^{\bullet-}$ production after 1 h of treatment (Fig. 10). $O_2^{\bullet-}$ production was evaluated during 6 h of treatment. The positive control (antimycin A) also increased fluorescence.

DISCUSSION

In the present study, the antitrypanosomal activity of BZTS against the epimastigote and trypomastigote forms of *T. cruzi* was evaluated. We found that this compound dose-dependently inhibited the growth of epimastigotes and reduced the viability of trypomastigotes. Based on the cytotoxicity assay in $LLCMK_2$ cells, BZTS was shown to be more toxic to the protozoa than to mammalian cells. Thiosemicarbazones constitute an important class of synthetic compounds with several pharmacological activities (Beraldo, 2004; Britta *et al*. 2012, *2014*).

The TEM analysis showed that BZTS induced substantial ultrastructural alterations, principally in mitochondria of the epimastigote form of *T. cruzi*, leading to swelling and the appearance of membranous structures in the organelle matrix. We also

https://doi.org/10.1017/S0031182015000141 Published online by Cambridge University Press

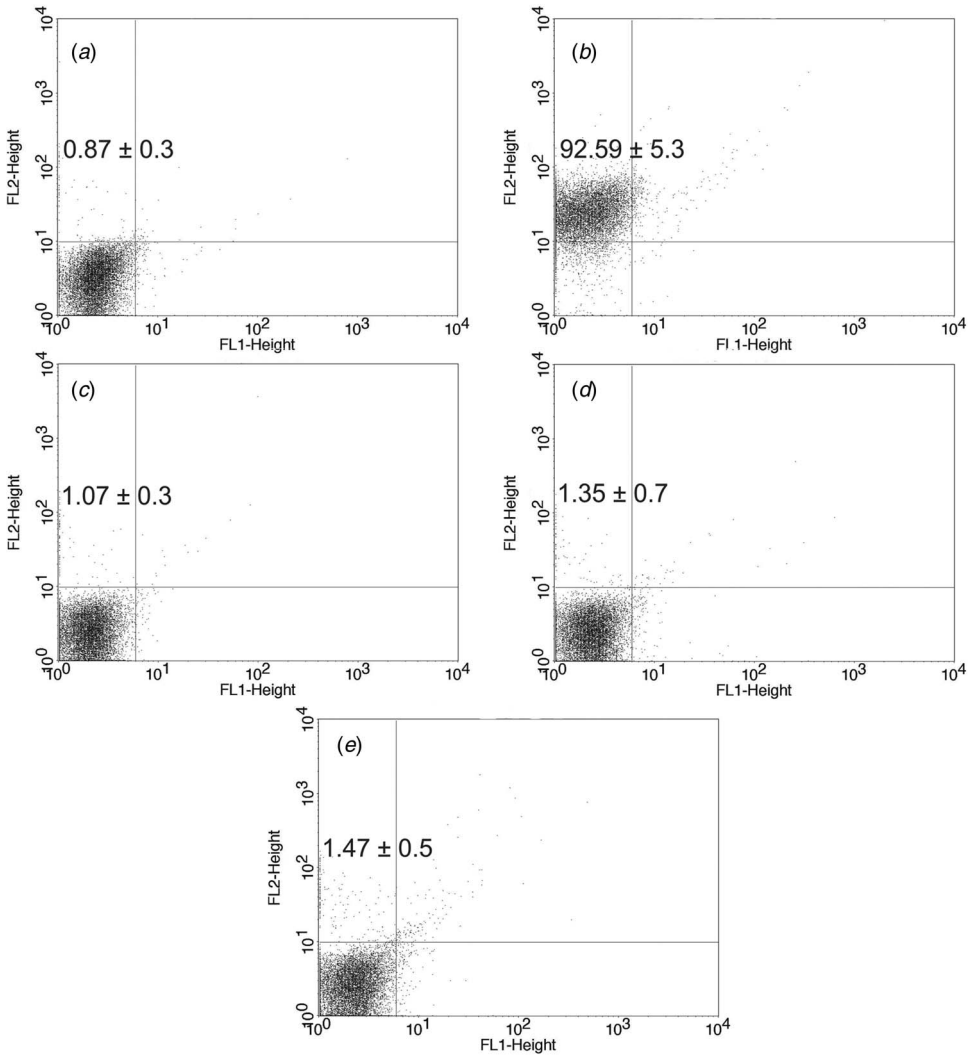

Fig. 6. *Trypanosoma cruzi* epimastigotes treated with BZTS and stained with PI. (A) Untreated epimastigotes. (B) Epimastigotes treated with digitonin. (C–E) Epimastigotes treated with BZTS at concentrations of 139 μM (C), 277 μM (D), and 555 μM (E). The percentage of PI-positive cells is shown in the upper-left quadrant.

detected autophagic characteristics, such as cytosolic membranous structures, the appearance of endoplasmic reticulum that surrounded organelles, and intense cytosolic vacuolization. Similar results were reported in epimastigotes of *T. cruzi* that were treated with naphthoquinones (NQs). Four NQs induced mitochondrial swelling, vacuolization, flagellar blebbing, the appearance of large endoplasmic reticulum profiles that surrounded different cellular structures, and myelin-like membranous contours. These morphological characteristics indicate an autophagic process (Salomão *et al*. 2013). Additionally, similar results were also observed in *Apis mellifera* venom-treated epimastigotes that showed an intense swelling of the mitochondria, with an altered inner mitochondrial membrane forming concentric membrane structures inside the organelle. Other remarkable feature was the presence of endoplasmic reticulum profiles surrounding different structures, suggesting autophagosome formation (Adade *et al*. 2012).

The TEM analysis revealed no plasma membrane damage in BZTS-treated epimastigotes. We also evaluated the integrity of the cell membrane using flow cytometry and PI to confirm that the plasma membrane was unaffected. Treatment with BZTS did not induce permeabilization of the plasma membrane compared with untreated parasites, confirming no interference with the cell membrane of the parasites.

The mitochondrion of trypanosomatid parasites is an important organelle that is distinct from mammalian mitochondria, making it an attractive target for antiprotozoal chemotherapy. Mitochondrial membrane potential is responsible for the formation and maintenance of oxidative phosphorylation, regulating the selectivity and permeability of the mitochondrial membrane to many types of material. In normal cells, the electrochemical gradient is maintained by active H^+ pumping during the transfer of electrons throughout the respiratory chain. Therefore, the membrane potential maintains the

https://doi.org/10.1017/S0031182015000141 Published online by Cambridge University Press

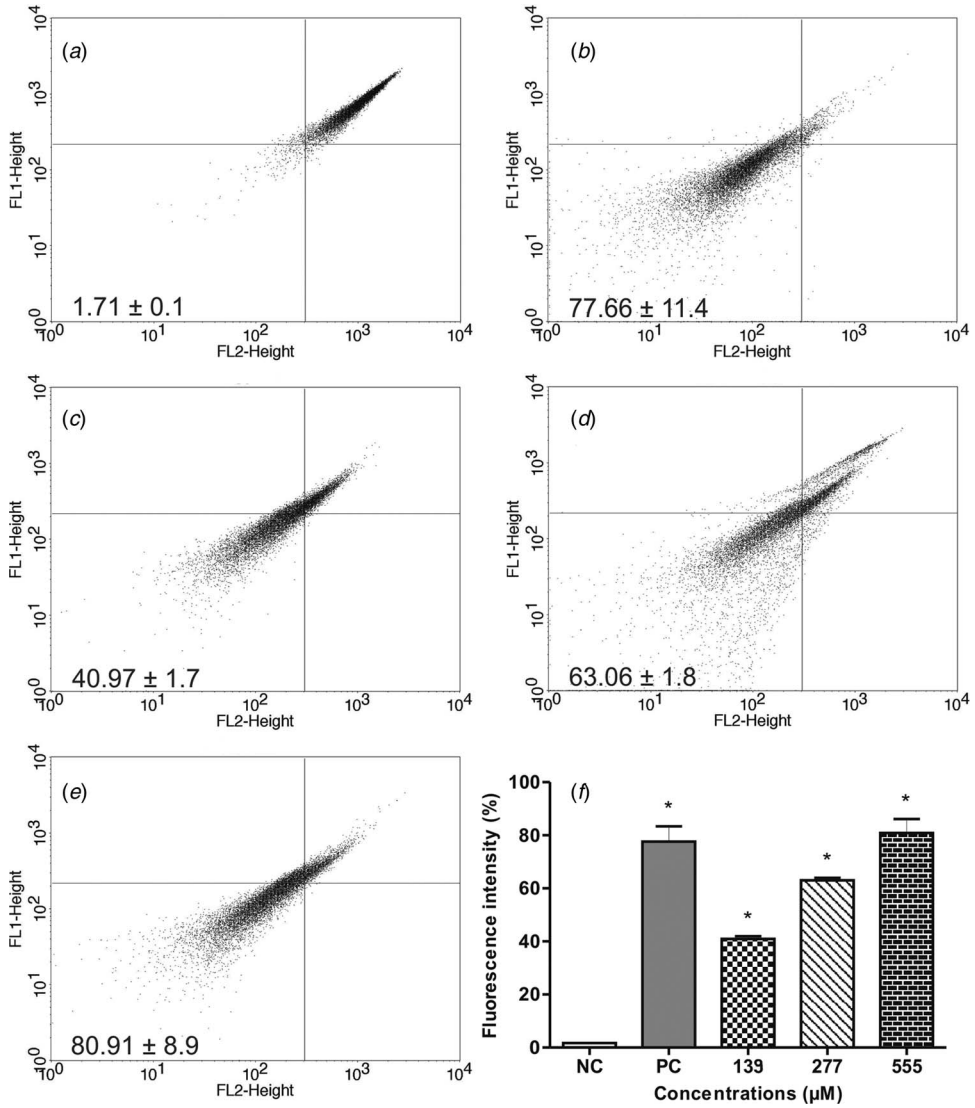

Fig. 7. Mitochondrial membrane potential assay using flow cytometry and rhodamine 123. (A) Untreated *T. cruzi* epimastigotes (negative control). (B) Epimastigotes treated with CCCP (positive control). (C–E) Epimastigotes treated with BZTS at concentrations of 139 μM (C), 277 μM (D), and 555 μM (E). FL1-H, rhodamine 123 fluorescence. The decrease percentage of Rh123 fluorescence is shown in the lower-left quadrant and summarized in F.

integrity and function of mitochondria. Alterations in the membrane potential can lead to a decrease in adenosine triphosphate production and a reduction of the translation and transcription of mitochondrial genes, ultimately resulting in apoptosis and/or necrosis (Shang *et al*. 2009; Sandes *et al*. 2014).

The TEM analysis suggested that BZTS exerted its antitrypanosomal activity by affecting mitochondrial function in the parasites. To determine whether BZTS changes the $\Delta\Psi$m in epimastigotes and trypomastigotes, we used Rh123, a cell-permeable, cationic, green-fluorescent dye that is readily sequestered by mitochondria with a normal $\Delta\Psi$m. The flow cytometry analysis of BZTS-treated parasites that were labelled with Rh123 showed a significant loss of the $\Delta\Psi$m, with a decrease in Rh123 fluorescence intensity. The reduced retention of Rh123 did not appear to be attributable to secondary plasma membrane permeabilization because the percentage of PI-labelled parasites after treatment was similar to untreated parasites. These results are consistent with the extensive damage of the parasite mitochondria as detected by TEM. Nevertheless, our results demonstrate that the alterations in the $\Delta\Psi$m that were caused by treating the parasites with BZTS preceded parasite cell death.

Our previous studies demonstrated the *in vitro* antileishmanial activity of benzaldehyde thiosemicarbazone derived from limonene complexed with copper against *L. amazonensis*, with an effect on mitochondrial function (Britta *et al*. 2012). Britta *et al*. (2014) also demonstrated that BZTS has potent antiproliferative activity against different evolutive forms of *L. amazonensis* and induced marked effects on the morphology and ultrastructure

https://doi.org/10.1017/S0031182015000141 Published online by Cambridge University Press

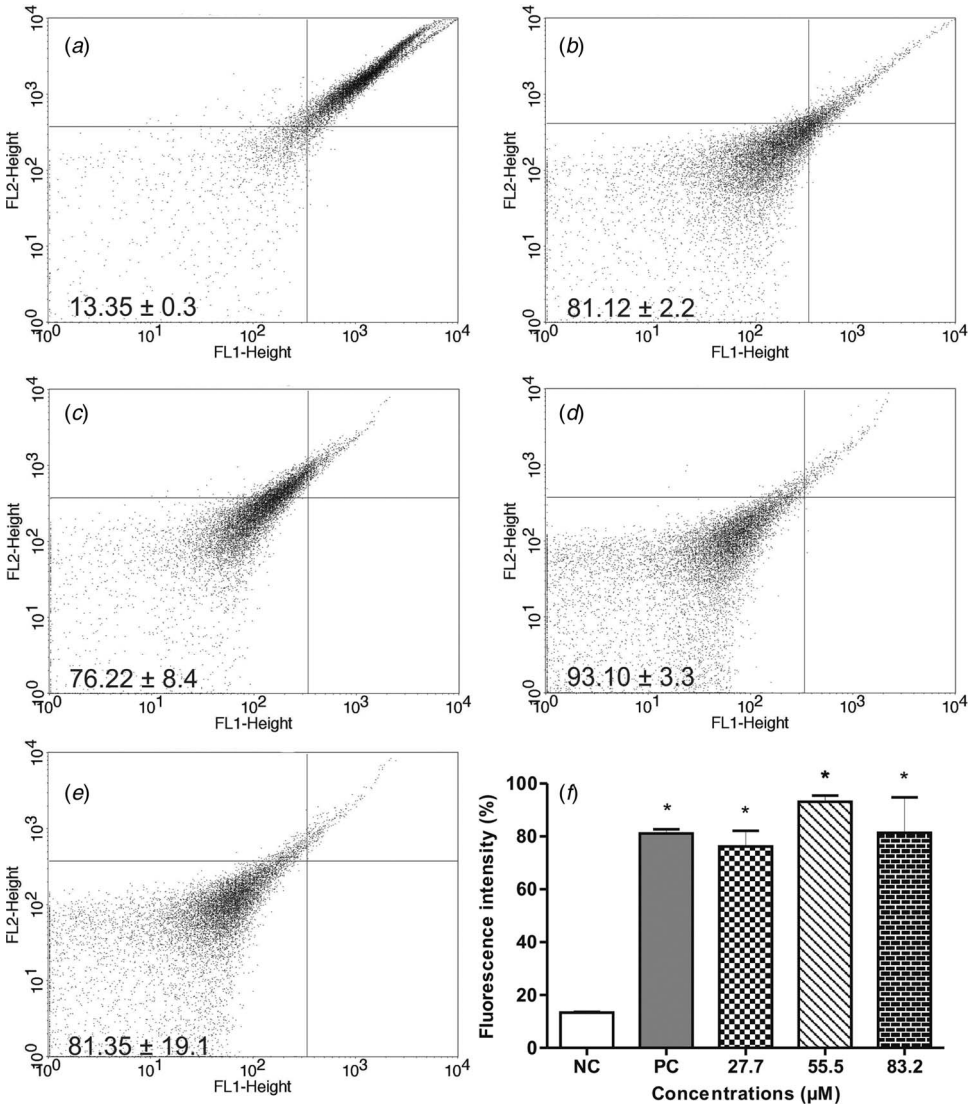

Fig. 8. Mitochondrial membrane potential assay using flow cytometry and rhodamine 123. (A) Untreated *T. cruzi* trypomastigotes (negative control). (B) Trypomastigotes treated with CCCP (positive control). (C–E) Trypomastigotes treated with BZTS at concentrations of 27·7 μM (C), 55 μM (D), and 83·2 μM (E). FL1-H, rhodamine 123 fluorescence. The decrease percentage of Rh123 fluorescence is shown in the lower-left quadrant and summarized in F.

of this parasite, such as interference with various cellular processes that led to changes in shape and mitochondrial function. Epimastigote forms of *T. cruzi* that were treated with 3-hydroxy-2-methylene-3-(4-nitrophenylpropanenitrile) (MBHA3) exhibited extensive plasma membrane damage, the loss of $\Delta\Psi$m, DNA fragmentation, and acidification of the cytoplasm, suggesting that MBHA3 at higher concentrations induces death by necrosis in a mitochondrion-dependent manner (Sandes *et al*. 2014). These authors suggested that MBHA3 molecules can induce the production of free radicals and reactive oxygen species (ROS), resulting in a decrease in $\Delta\Psi$m and cell death. Because of the absence of efficient mechanisms for ROS detoxification in these parasites, mitochondria appear to be a good target for drug intervention (Soeiro and De Castro, 2009). *Apis mellifera* venom-treated epimastigotes and trypomastigotes also showed gradual decreases in Rh123 median fluorescence emission, suggesting interference in the proton electrochemical potential gradient membrane (Adade *et al*. 2012).

The present study found that BZTS induced mitochondrial dysfunction that causes enhanced $O_2^{\bullet-}$, and that is major cause of the cellular oxidative damage. These effects were also previously reported in BZTS-treated *L. amazonensis* (Britta *et al*. 2014). Edelfosine treatment altered the ultrastructure of mitochondria, followed by changes in $\Delta\Psi$m using Rh123 and flow cytometry analysis, which likely indicates apoptosis-like cell death (Santa-Rita *et al*. 2004).

In conclusion, we found that BZTS exerted antiproliferative, ultrastructural and physiological effects on epimastigote and trypomastigote forms of *T. cruzi*. BZTS is able to cause detrimental effects in parasites that are mainly related to the ultrastructure and physiology of mitochondria,

https://doi.org/10.1017/S0031182015000141 Published online by Cambridge University Press

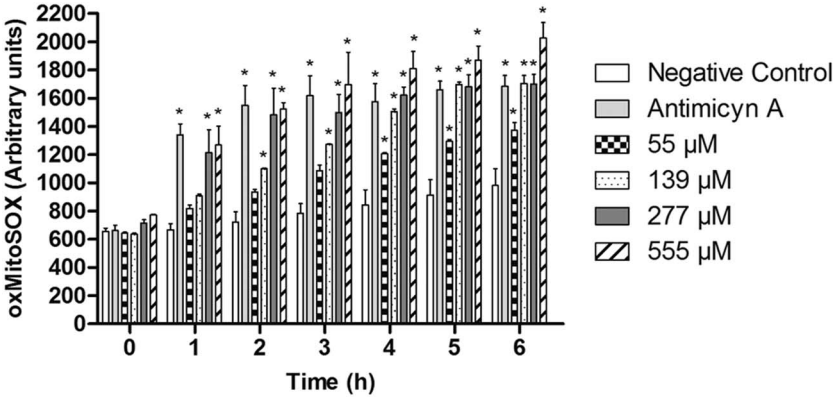

Fig. 9. Mitochondrial $O_2^{\bullet-}$ production in *T. cruzi* epimastigotes treated with 55, 139, 277 and 555 μM BZTS for up to 6 h using the fluorescence probe MitoSOX. Antimycin A (10 μM) was used as a positive control. Fluorescence was measured with a VICTOR X3 spectrofluorometer (Perkin-Elmer). The results are expressed as the mean ± S.E. of MitoSOX oxidation (arbitrary units) of at least three independent experiments. $*P \leq 0{\cdot}05$, significant difference from negative control group.

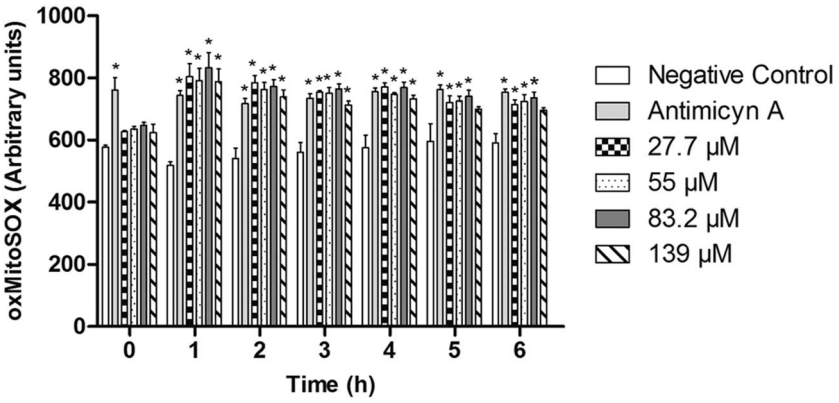

Fig. 10. Mitochondrial $O_2^{\bullet-}$ production in *T. cruzi* trypomastigotes treated with 27·7, 55, 83·2 and 139 μM BZTS for up to 6 h using the fluorescence probe MitoSOX. Antimycin A (10 μM) was used as a positive control. Fluorescence was measured with a VICTOR X3 spectrofluorometer (Perkin-Elmer). The results are expressed as the mean ± S.E. of MitoSOX oxidation (arbitrary units) of at least three independent experiments. $*P \leq 0{\cdot}05$, significant difference from negative control group.

which could be closely related to parasite death through distinct cell death pathways.

AKNOWLEDGEMENTS

This work was supported by the Conselho Nacional de Desenvolvimento Cientifico e Tecnológico (CNPq), Fundação de Aperfeiçoamento de Pessoal de Nível Superior (CAPES) and Instituto Nacional de Ciência e Tecnologia para Inovação Farmacêutica (INCT-*if*).

REFERENCES

Adade, C. M., Chagas, G. S. and Souto-Padron, T. (2012). *Apis mellifera* venom induces different cell death pathways in *Trypanosoma cruzi*. *Parasitology* **139**, 1444–1461.

Álvarez, J. M., Fonseca, R., Borges Da Silva, H., Marinho, C. R., Bortoluci, K. R., Sardinha, L. R. and D'império-Lima, M. R. (2014). Chagas disease: still many unsolved issues. *Mediators of Inflammation* **2014**. 9 pages. doi: 10.1155/2014/912965.

Beraldo, H. (2004). Semicarbazones and thiosemicarbazones: their wide pharmacological profile and clinical applications. *Química Nova* **27**, 461–471.

Bombeiro, A. L., Gonçalves, L. A., Penha-Gonçalves, C., Marinho, C. R. F., Lima, M. R. D. I., Chadi, G. and Álvarez, J. M. (2012). IL-12p40 deficiency leads to uncontrolled *Trypanosoma cruzi* dissemination in the spinal cord resulting in neuronal death and motor dysfunction. *PLoS ONE* **7**, e49022.

Britta, E. A., Silva, A. P. B., Ueda-Nakamura, T., Dias-Filho, B. P., Silva, C. C., Sernaglia, R. l. and Nakamura, C. V. (2012). Benzaldehyde thiosemicarbazone derived from limonene complexed with copper induced mitochondrial dysfunction in *Leishmania amazonensis*. *PLos ONE* **7**, e41440.

Britta, E. A., Scariot, D. B., Falzirolli, H., Ueda-Nakamura, T., Dias-Filho, B. P., Silva, C. C., Borsali, R. and Nakamura, C. V. (2014). Cell death and ultrastructural alterations in *Leishmania amazonensis* caused by new compound 4-nitrobenzaldehyde thiosemicarbazone derived from S-limonene. *BMC Microbiology* **14**, 236.

Cerecetto, H. and González, M. (2002). Chemotherapy of Chagas' disease: status and new developments. *Current Topics in Medicinal Chemistry*, **2**, 1187–1213.

Coura, J. R. and De Castro, S. L. A. (2002). Critical review on Chagas Disease chemotherapy. *Memórias do Instituto Oswaldo Cruz* **91**, 3–24.

De Souza, W., De Carvalho, T. M. U. and Barrias, E. S. (2010). Review on *Trypanosoma cruzi*: host cell interaction. *International Journal of Cell Biology* **2010**, 18 pages. doi: 10.1155/2010/295394.

Kransdorf, E. P., Zakowski, P. C. and Kobashigawa, J. A. (2014). Chagas disease in solid organ and heart transplantation. *Current Opinion in Infectious Diseases* **27**, 418–424.

Salomão, K., De Santana, N. A., Molina, M. T., De Castro, S. L. and Menna-Barreto, R. F. (2013). *Trypanosoma cruzi* mitochondrial swelling and membrane potential collapse as primary evidence of the mode of action of naphthoquinone analogues. *BMC Microbiology* **13**, 196.

Sandes, J. M., Fontes, A., Regis-Da-Silva, C. G., De Castro, M. C. B., Lima-Junior, C. G., Silva, F. P., Vasconcellos, M. L. A. A. and Figueiredo, R. C. (2014). *Trypanosoma cruzi* cell death induced by the Morita-Baylis-Hillman Adduct 3-Hydroxy-2-Methylene-3-(4-Nitrophenylpropanenitrile). *PloS ONE* **9**, e93936.

Santa-Rita, R. M., Henriques-Pons, A., Barbosa, H. S. and De Castro, S. L. (2004). Effect of the lysophospholipid analogues edelfosine, ilmofosine and miltefosine against *Leishmania amazonensis*. *Journal of Antimicrobial Chemotherapy* **54**, 704–710.

Shang, X. J., Yao, G., Ge, J. P., Sun, Y., Teng, W. H. and Huang, Y. F. (2009). Procyanidin induces apoptosis and necrosis of prostate cancer cell line PC-3 in a mitochondrion-dependent manner. *Journal of Andrology* **30**, 122–126.

Soeiro, M. N. C. and De Castro, S.l. (2009). *Trypanosoma cruzi* targets for new chemotherapeutic approaches. *Expert Opinion on Therapeutic Targets* **13**, 105–121.

Vannucchi, V., Tomberli, B., Zammarchi, L., Fornaro, A., Castelli, G., Pieralli, F. and Olivotto, I. (2015). Chagas disease as a cause of heart failure and ventricular arrhythmias in patients long removed from endemic areas: an emerging problem in Europe. *Journal of Cardiovascular Medicine*. doi: 10.2459/JCM.0000000000000045.

World Health Organization (2014). *Chagas Disease (American Trypanosomiasis)*. Fact Sheet 340. World Health Organization, Geneva, Switzerland.